Sorption and Ordering of Dibranched Alkanes on Medium-Pore Zeolites Ferrierite and TON

Johannis A. Z. Pieterse,[†] Sheila Veefkind-Reyes,[†] K. Seshan,[†] and Johannes A. Lercher*[,†,‡]

Faculty of Chemical Technology, University of Twente, P.O. Box 217, 7500 AE Enschede, The Netherlands, and Institut für Technische Chemie, Technische Universität München, Lichtenbergstrasse 4, D-85748 Garching, Germany

Received: November 9, 1999; In Final Form: March 3, 2000

The sorption of (methyl-substituted) pyridines and 2,2-dimethylalkanes on the medium-pore zeolites FER and TON has been studied by in situ IR spectroscopy, calorimetry, and gravimetry in order to describe sorption at the outer surface and the pore mouths of the zeolite crystals. Six percent and 3% of the Brønsted acid sites (determined by adsorption of 2,4,6-trimethylpyridine) were found to be on the outer surface and the pore mouth of TON and FER, respectively. This result agrees fairly well with the fraction of sites that are available for the 2,2-dimethylalkanes, which are unable to fully enter the pores of the zeolites studied. Remarkably, at low coverage, all three dimethylalkanes adsorb in parallel to the outer surface. As the coverage increases, additional 2,2-dimethylpentane and 2,2-dimethylhexane molecules sorb in such a manner that the propyl and butyl groups point into the pore. Also, approximately 80% of the 2,2-dimethylpentane and 2,2-dimethylhexane molecules that initially sorbed parallel to the outer surface rearrange to this sorption structure. This ordering is well documented by the marked increase in the heat of adsorption as the equilibrium pressure increases and by the IR spectra of hydroxyl groups in interaction with the alkane during this process.

Introduction

Ferrierite (FER) and ZSM-22 (TON), in their proton-exchanged forms, are catalysts commercially applied in the skeletal isomerization of alkenes and alkanes.[1,2] Although the heuristic aspects of the catalytic properties of both molecular sieves are well documented, the mechanistic aspects of the conversions on a molecular level are remarkably controversial.

The pore diameters of TON and FER are similar to the kinetic diameters of singly branched alkanes. Thus, it is difficult to imagine that the total volume of the molecular sieve is utilized for the reaction. The shapes of the pores and the molecules suggest that individual molecules cannot pass each other within a channel, i.e., single-file diffusion prevails.[3] The severe impact of these constraints on the microscopic steps of sorption and surface reaction led Martens et al. to conclude that skeletal isomerization of hexadecane proceeds only at the pore mouth and the outer surface of TON crystallites.[4] It was shown that the array of adjacent pore openings acts as a template for the branching of the linear chain. The spacing of the pores in the crystal surface and the chain branching in the hydrocarbon skeletons match closely.

Although such a concept is intuitively intriguing, it is mainly based on circumstantial kinetic evidence. Very little is known about the nature and morphology of the outer surface of zeolites. The proposed concept assumes a clean and mesoscopically uncorrugated surface, providing the regularity needed for the linear chain to isomerize in regular intervals. As one synthesizes a microporous material out of a solution containing colloidal or dissolved silica entities, it is unlikely that the surface is not contaminated by amorphous material that forms a macroporous overlayer. This is expected to severely impact the sorption of sterically more demanding alkanes. Moreover, it is frequently found that the distribution of alumina is inhomogeneous over the crystallite, and hence, the concentration of Brønsted acid sites cannot be deduced by extrapolating the bulk chemical composition. Thus, the concentration, strength, and accessibility of Brønsted acid sites at the pore entrance must be assessed experimentally in order to allow for a full molecular description of the sorption and eventually of the zeolite-catalyzed reactions.

In this contribution, we describe the unique sorption behavior of dibranched alkanes on FER and TON, serving as a model for the manner in which sterically demanding molecules might sorb on the surface of microporous materials. Additionally, a quantitative determination of the concentration of acid sites in FER and TON accessible to reactants of various sizes is discussed.

Experimental Section

Materials. Silica (Aerosil 200) was obtained from Degussa. For activation, the material was heated in a vacuum at a rate of 10 K min^{-1} to 873 K and held at that temperature for 1 h. NH_4^+-ZSM22 with a Si/Al ratio of 52:1 was received from Dr. M. Derewinski of the Polish Academy of Science. Na/K-FER was obtained from Tosoh Corporation (Si/Al, 9:1). The samples were completely transformed into the NH_4^+ form by ion exchanging them three times with 1 *m* NH_4NO_3. The NH_4^+ form was transformed to the H^+ form by heating in a vacuum to 673 K at a rate of 10 K min^{-1}. Pyridine and 2,4,6-trimethylpyridine (TMP) were obtained from Fluka (>99% purity). 2,2-Dimethylbutane (DMB), 2,2-dimethylpentane (DMP), and 2,2-dimethylhexane (DMH) were obtained from Sigma Aldrich (>99.95% purity).

* To whom correspondence should be addressed. Telephone: +49-89-28913540. Fax: +49-89-28913544. E-mail: johannes.lercher@ch.tum.de.
[†] University of Twente.
[‡] Technische Universität München.

10.1021/jp993965h CCC: $19.00
Published on Web 05/31/2000

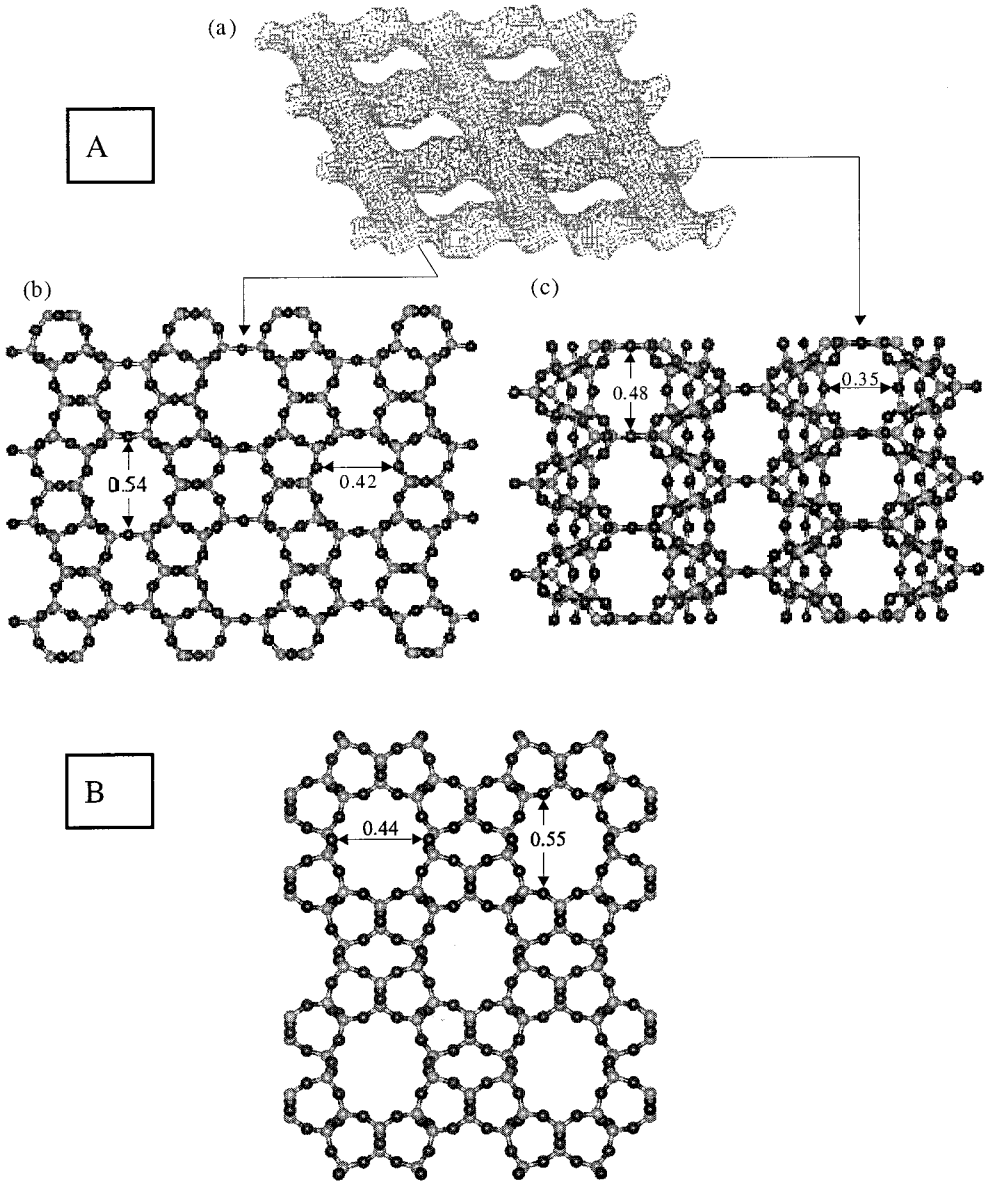

Figure 1. (A) Schematic representation of FER: (a) pore system, b) view along the 10-ring channels, and c) view along the 8-ring channels). (B) Schematic representation of TON, viewed along the 10-ring channels.

Infrared Spectroscopy. The adsorption studies were performed in a vacuum infrared cell, which was placed in a Bruker IFS88 IR spectrometer. The cell was evacuated to a base pressure of 10^{-7} mbar. The samples were pressed into self-supporting wafers with concentrations of approximately 3 mg/cm^2 and activated in situ at 673 K. The probe molecules were introduced via a differentially pumped dosing valve. The partial pressure was increased stepwise from 10^{-4} to 10^{-1} mbar. The integrated intensities of a band characteristic of pyridinium ions and the decrease in the intensity of the hydroxyl bands were used to determine the fraction of Brønsted acid sites accessible. Comparative measurements on silica were used to assign the bands for the substituted pyridines. Detailed information on the experimental procedures can be found in refs 5 and 22.

Microcalorimetry and Gravimetry. The gravimetric and calorimetric measurements were performed in a modified SETARAM TG-DSC 111 instrument.[5] The system consists of four main parts, i.e., the balance, the calorimeter, the vacuum system, and the mass spectrometer for analyzing the gas composition. For the sorption experiments, the samples were pressed into thin wafers that were subsequently broken into small platelets. As described above, the NH_4^+ form of the samples was transformed into the H^+ form by heating in a vacuum to 673 K with an increment of 10 K min^{-1} and holding that temperature for 2 h. After activation, the system was cooled to the sorption temperature. The adsorption of dibranched alkanes was studied at 343 K between 10^{-2} and 13 mbar equilibrium pressure. The hydrocarbons were admitted in doses and were allowed to equilibrate with the zeolite. Equilibration was assumed to be reached when the heat signal reached the initial, constant value and changes in the gravimetric signal were not observed. NH_3 sorption measurements were performed in order to determine the total acid site concentration.

Results and Discussions

Structural Information and General Characterization. FER contains two perpendicularly intersecting channel systems.[6,7] One consists of 10-membered rings with dimensions of 0.42 × 0.54 nm, the other of eight-membered rings with dimensions of 0.35 × 0.48 nm (see Figure 1A). The unit cell is reported to contain five nonequivalent T atoms.[7] The density of T atoms is reported to be 17.7 per 1000 Å^3.[6]

TABLE 1: Maximum Uptake with Pyridine and TMP at 298 and 573 K

	coverage at 10^{-4} mbar (%)		coverage at 10^{-3} mbar (%)		coverage at 10^{-2} mbar (%)		coverage at 10^{-1} mbar (%)	
probe molecule	TON	FER	TON	FER	TON	FER	TON	FER
2,4,6-trimethylpyridine	3	1	5	2.5	6	3	–	–
pyridine	43	27	59	40	92	45 (69)[a]	100[a]	100[a]

[a] At 573 K.

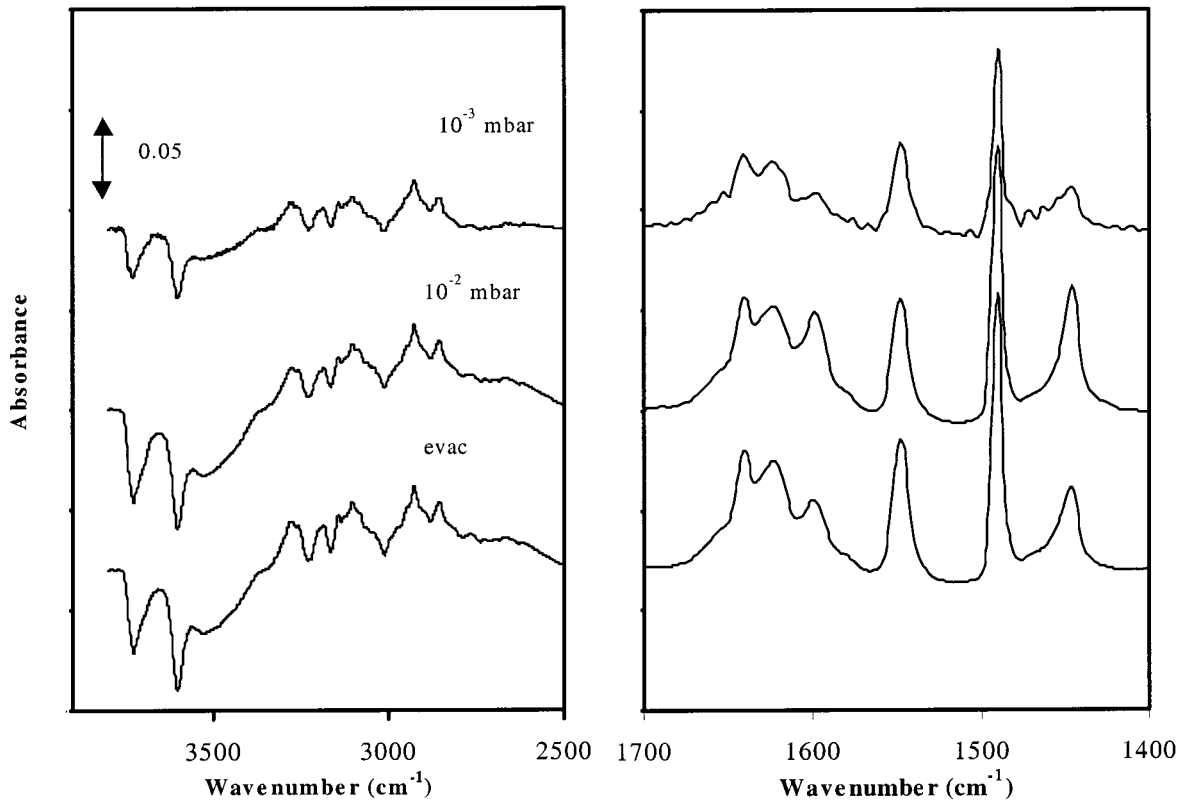

Figure 2. Sorption of pyridine on TON at room temperature and 10^{-3} and 10^{-2} mbar equilibrium loading.

The TON structure has a unidimensional elliptical pore system. The channels consist of 10-membered rings and have dimensions of 0.44 × 0.55 nm (see Figure 1B). The density of T atoms is reported to be 19.7 per 1000 Å^3.[6]

Scanning electron microscopy (SEM) showed small platelike particles for FER, with sizing (1−2) × 1 μm. For TON, a needlelike structure was observed, with sizing (2−4) × 1 μm. By means of ammonia and pyridine sorption [$\epsilon(1455) = 1.5$ μmol^{-1} cm, and $\epsilon(1545) = 1.8$ μmol^{-1} cm [8]], the Brønsted acid site concentrations of FER and TON were determined to be 1.19 mmol/g and 0.36 mmol/g, respectively. The Lewis acid site concentrations were estimated to be 0.07 mmol/g and 0.05 mmol/g, respectively. The heat of ammonia sorption was 140 kJ/mol in both cases, indicating a similar strength of interaction between the acid sites of the materials and the sorbed ammonia.

Adsorption of Pyridine Homologues. The probe molecules used in this study were pyridine and 2,4,6-trimethylpyridine (TMP). The size of TMP, 6.2 × 5.6 Å, clearly suggests that the sorption of TMP allows for calibration of the concentration of the acid sites at the external surface and in the micropore mouth. Sorption of the pyridines on Brønsted acid sites leads to the formation of pyridinium ions and to hydrogen-bonded pyridine.[8−11] The interaction of the nitrogen lone pair with accessible Al^{3+} cations leads to an electron pair donor−electron pair acceptor type of interaction (interaction with Lewis sites). The basicity of pyridines increases with methyl substitution because of inductive effects; however, it is known that substitution in positions 2 and 6 induces steric constraints at the nitrogen lone pair, weakening the coordination compared to that of pyridine.[10] This prompted Benesi et al. to propose the use of 2,6-dimethylpyridine as a specific probe for protonic sites.[12] Although the molecule was used subsequently for selectively poisoning Brønsted acid sites,[13] Knözinger et al. showed that TMP is able to form coordinative bonds with exposed aluminum cations on a γ-alumina surface.[10]

Adsorption on TON. For TON, sorption studies were carried out at 298 K with pyridine and TMP. Typically, the compounds were sorbed at 10^{-4} mbar, allowed to equilibrate, and stepwise exposed to pressures of 10^{-3} and 10^{-2} mbar. The maximum fraction of Brønsted acid sites consumed after equilibration at the different partial pressures of pyridine and TMP are compiled in Table 1. The maximum loading was 6% for TMP and 92% for pyridine. Figure 2 shows the difference IR spectra obtained for pyridine after equilibration for the loadings studied. Upon admittance of pyridine, the band at 3740 cm^{-1} disappeared completely (all SiOH were fully accessible), while the band of bridging OH groups at 3603 cm^{-1} disappeared only in part. The strong and broad absorption band between 3300 and 2000 cm^{-1} indicates moderately strong hydrogen bonding of pyridine with the Si−OH groups and of pyridinium ions with the bridging oxygen at the aluminum framework sites. With an increase in the partial pressure of pyridine, the interaction with the zeolite framework (conjugated weak base) is partly replaced by the interaction with excess pyridine, as concluded from the ad-

TABLE 2: Assignment of Vibrational Modes of Pyridine (Py) and TMP Adsorbed on FER and TON[a]

vibrational mode[b]	Py liquid[c]	PyH^+ [c]	PyL[c]	TMP on γ-alumina[d]	$TMPyH^+$ [c]	TMPyL[b]
8a; $\nu_{CC}(N)A_1$	1579 s	1638 s (1640 s)	(1600 m)	1634	1639 vs (1637 m)	–
8b; $\nu_{CC}(N)B_1$	1572 m	1619 s (1623 s)	(1575 m)	1566	1572 w (1574 m)	–
19a; $\nu_{CC}(N)A_1$	1478 s	1489 vs (1491 vs)	–	1500	1488 w	–
δ_{as,CH_3}	–	–	–	1455	–	1452 w
19b; $\nu_{CC}(N)B_1$	1439 vs	1545 s (1547 s)	1455 w (1456 m)	1415	1547 w	1411 w
δ_{s,CH_3}	–	–	–	1383	1390 w	1380 w

[a] Values in parentheses represent TON. [b] Ref 11, denotes ring vibrations following symmetry selection rules (applied to point group of pyridine). [c] Notation: vs, very strong; s, strong; m, medium; w, weak. [d] Ref 10.

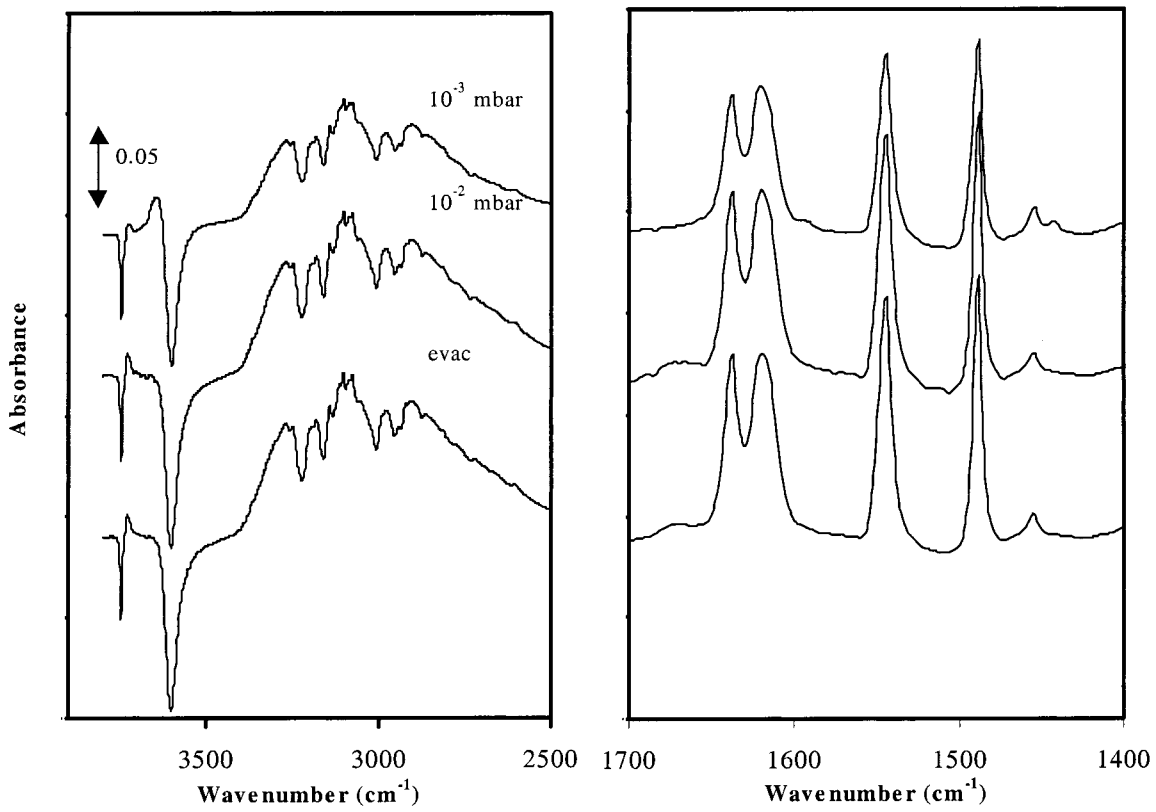

Figure 3. Sorption of pyridine on FER at room temperature and 10^{-3} and 10^{-2} mbar equilibrium loading.

ditional perturbations of the N−H stretching vibrations of the pyridinium ions. The skeletal combination modes (overtones of the lattice vibrations) shifted to slightly lower wavenumber upon exposure to pyridine. Ring vibration bands were observed at 1640, 1623, 1600, 1547, 1494, 1456, and 1446 cm^{-1}. Through a comparison of these values with the results reported by Glazunov et al.,[14] these bands were assigned to ring-stretching modes [1640, 1623, 1547, 1491 (PyH^+), 1600, and 1491 cm^{-1}(PyL)]. The band at 1547 cm^{-1} served as a characteristic band for quantifying pyridinium ions (PyH^+). To quantify pyridine adsorbed coordinatively to accessible Al^{3+} cations (PyL), the band at 1456 cm^{-1} was used, and for physisorbed pyridine, the band at 1446 cm^{-1} was used. Detailed assignments on the basis of refs 10, 11, and 14−18 are compiled in Table 2.

The equilibrium coverage of TMP was significantly lower than that of pyridine. All Si−OH groups interacted with TMP. However, only 6% of the strong Brønsted acid sites (3604 cm^{-1}) disappeared after equilibration at 10^{-2} mbar. In parallel, a band at 1637 cm^{-1} corresponding to $TMPH^+$ appeared. The low uptake indicates that only the outer surface and the pore mouths are accessible for TMP. In accordance with ref 8, the sole presence of $TMPH^+$ is attributed to the steric constraints around the nitrogen atom. To test the accessibility of acid sites under relevant catalytic conditions, pyridine was sorbed at 573 K and 10^{-1} mbar. Despite the large differences at low temperatures, pyridine covered nearly 100% of the strong Brønsted acid sites, as concluded from the complete disappearance of the band of the SiOHAl groups (Table 1).

Adsorption on FER. Table 1 shows the uptake of pyridine and TMP after 21 h of contact with 10^{-4}, 10^{-3}, and 10^{-2} mbar of the sorbate at room temperature. It was not possible to reach equilibrium coverage with pyridine at the low pressures despite the extended equilibration time (21 h). Therefore, coverages are compared at 10^{-2} mbar after 21 h. In the case of pyridine, 45% of all Brønsted acid sites were concluded to interact after 21 h of equilibration time. The slow equilibration is affiliated with greater acid site density and slightly smaller 10-membered ring openings of FER in comparison with TON. TMP reached only 3% of all Brønsted acid sites. In the case of TMP sorption, the band corresponding to $TMPH^+$ appeared at 1638 cm^{-1} and persisted upon evacuation at ambient temperature. Other bands at 1617 and 1570 cm^{-1} (TMP coordinated to a Lewis acid site) disappeared upon evacuation, indicating that coordinatively bound TMP is not stable at 10^{-7} mbar at ambient temperature.

Figure 3 shows the (difference) IR spectra for pyridine at

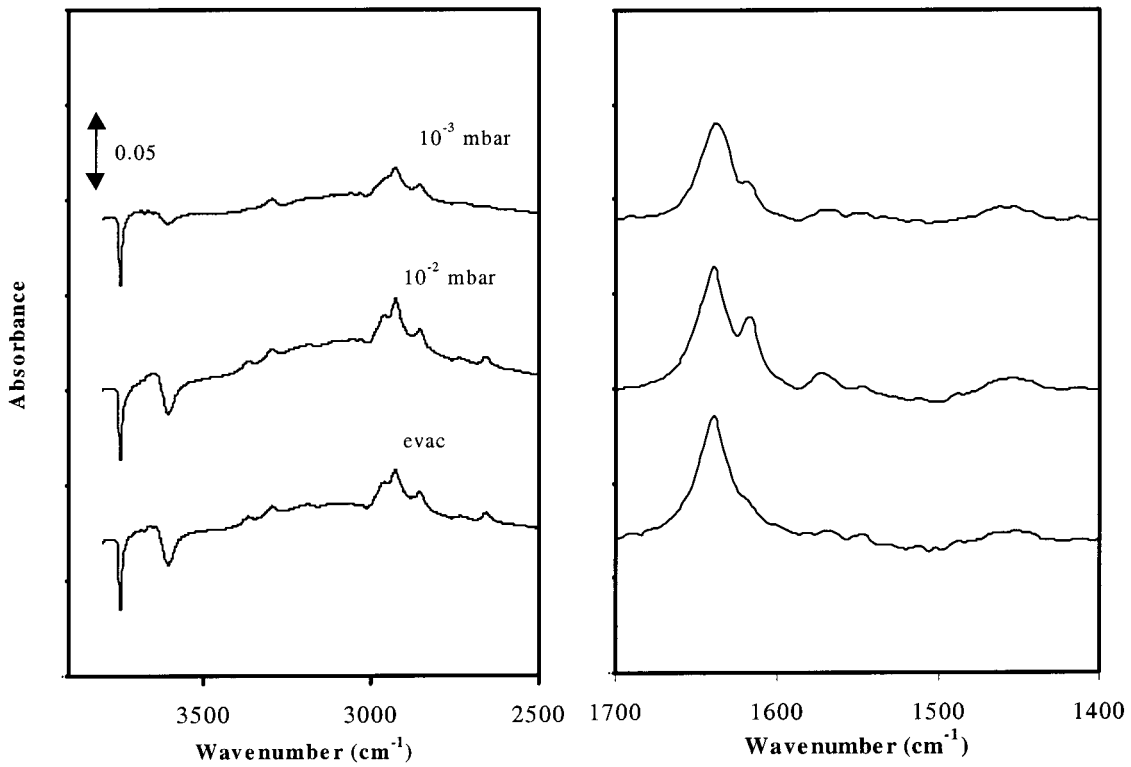

Figure 4. Sorption of TMP on FER at room temperature and 10^{-3} and 10^{-2} mbar equilibrium loading.

298 K after 21 h of exposure. In accordance with its chemical composition, a greater intensity of the bands at 1619 and 1545 cm^{-1} and the smaller band at 1455 cm^{-1} indicate that FER has a greater concentration of Brønsted acid sites than TON. Upon contact with (substituted) pyridine (see also Figure 4for TMP), the band of the Si−OH groups is shifted downward by approximately 100 cm^{-1}, which is attributed to a weak hydrogen bonding via π electrons of the aromatic ring.[8] As this is the weaker basic function, it should be emphasized that only steric constraints can force pyridine not to interact via its lone electron pair at the nitrogen.

With increasing exposure to pyridine, the intensities of the bands characteristic of pyridinium ions and coordinatively adsorbed pyridine increased; however, their relative ratio remained the same. At the lowest loading, a substantially greater fraction of pyridine is bound to acid sites at the outer surface of the crystallites; thus, the monotonic change of relative intensities of the bands suggests an even distribution of Brønsted and Lewis acid sites throughout the material.

To probe the role of the temperature on the accessibility of the pore structure, pyridine was sorbed at 10^{-2} mbar and 573 K. Even at this higher temperature, equilibrium does not seem to be reached completely. After 42 h, 70% of the Brønsted acid sites interacted with the base, which is, however, substantially greater than the 45% found after exposure for 21 h at ambient temperature. To probe whether the limited coverage is related to constraints in accessiblity or to constraints in the transport of pyridine in FER, the sample was exposed to 10^{-1} mbar of pyridine at 573 K. In this case, full coverage was achieved after 73 h of exposure (Figure 5).

Sorption of Dibranched Alkanes. Interactions based on London dispersion forces and localized induced-dipole acid−base hydrogen bonding will contribute to the sorption of an alkane in a zeolite pore and on the outer surface of the crystallite.[20] The induced-dipole acid−base hydrogen bonding with alkanes has been shown to contribute only 6 kJ/mol for

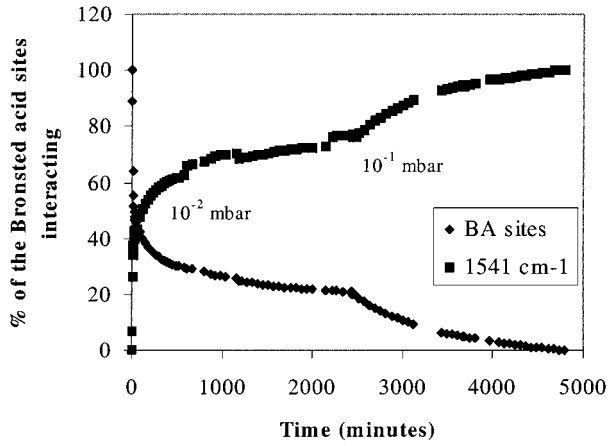

Figure 5. Uptake of pyridine on FER at 573 K.

FAU and 10 kJ/mol for H-ZSM5, independent of the size of the *n*-alkane. This should be compared with the overall heats of adsorption of *n*-hexane on H-FAU and H-ZSM5, which are 53 and 82 kJ/mol, respectively. This indicates that, for nonpolar and weakly polarizable molecules, the energy of interaction and the heat of sorption are energetically fairly well described with nonlocalized bonding.

The bonding forces involved are mostly determined by the geometry of the environment around the sorbed molecule. As these forces are additive, the strong interaction of weakly polar molecules in microporous materials has been explained by optimized interactions through the curved surface (see, e.g., the formulation of the "confinement effect" by Derouane[21]). Previous work of ours has shown that the concept agrees very well with experimental observations.[5,22,23] The heat of sorption depends subtly on the fit between the size of the molecule and the size of the zeolite pores. For light alkanes (ethane to *n*-hexane), the sorption enthalpy increases in the sequence FAU < MOR < MFI < TON. Usually, with FER, a 1−2 kJ/mol lower sorption enthalpy was found than with TON. This has

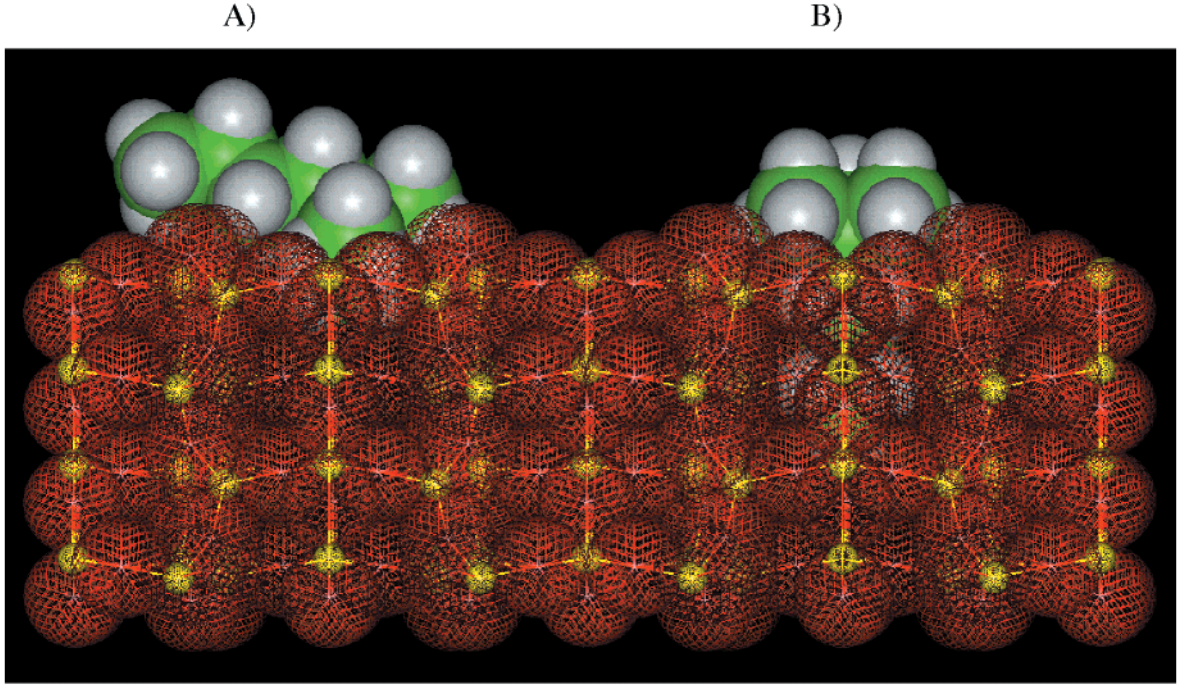

Figure 6. Optimized sorption structure of 2,2-dimethylhexane: (A) methyl group penetrating the pore mouth (18 kJ/mol) and (B) longer hydrocarbon-chain part penetrating the pore mouth (65 kJ/mol).

been attributed to increasing repulsive forces as the pore diameter passes an optimum value.[5] It should be noted that TON and FER exert constraints on the sorption of singly branched alkanes, leading to a lower uptake compared to *n*-alkanes. Therefore, sorption of dibranched alkanes allows one to probe selectively the sorption characteristics of the outer surface and pore entrance of TON and FER.

Model visualizations using MSI Insight II software support this conclusion.[27] A rigid fragment of SiO_2 polymorph with TON topology was generated using the crystallographic data from ref 6. Geometry optimization of 2,2-dimethylhexane was performed in a CVFF-aug force field, representative of the Lennard-Jones adsorption potential, in a vacuum until a RMS gradient (total energy gradient calculated as a root-mean-square gradient) of 10^{-4} kJ/mol was reached. The docking results suggest that the sorption structure of the molecule can be optimized at the outer surface in such way that the methyl group of the neopentane unit points into the pore mouth and the rest of the molecule is stretched along the surface (Figure 6A). Additionally, the molecule may pin the neopentane unit into the pore mouth with its butane tail pointing upward (not shown). Both sorption structures reveal similar adsorption potentials (18−24 kJ/mol). Finally, the molecule may enter the pore mouth with the longer hydrocarbon chain part, favorably in its most open (symmetric) conformation, with part of the neopentane unit remaining external to the pore (Figure 6B.). This results in an adsorption potential of about 65 kJ/mol.

Figure 7 depicts the heats of sorption of DMB, DMP, and DMH on TON, as a function of the sorbate loading at 343 K. For DMB, the heat of sorption was about 30 kJ/mol until a coverage of approximately 0.015 mmol/g was reached. At higher coverages, the very slow uptake at longer equilibration times indicates a rearrangement of molecules that produces a heat flux that is too low to be monitored by the calorimetric measurements.

Upon exposure of TON to DMP, the initial heat of sorption was about 25 kJ/mol. This value rapidly increased with coverage and reached 97 kJ/mol at a coverage of approximately 0.017 mmol/g. With further increases in coverage, the heat of adsorption dropped again to approximately 20 kJ/mol at a coverage of 0.05 mmol/g. A similar trend was found for DMH. The initial heat of adsorption was about 27 kJ/mol, and the maximum value of 113 kJ/mol was reached at a coverage of approximately 0.025 mmol/g.

For FER, very similar trends were observed as a function of coverage. The heat of sorption of DMB was again much lower than that of the other analogues. The highest value observed was 30 kJ/mol, but as with TON, a distinct maximum in the heat of adsorption was not observed. However, for DMP and DMH, the heat of adsorption increased again rapidly with coverage to maximum values of 95 and 108 kJ/mol, reached at coverages of 0.018 and 0.02 mmol/g, respectively (see Figure 7). If we assume that the uptake corresponds only to localized adsorption at the Brønsted acid sites, the maximum concentrations of acid sites involved in the local adsorption with DMB, DMP, and DMH can be estimated to be approximately 3, 5, and 5.5%, respectively, for TON and 1, 2, and 2.5%, respectively, for FER.

It should be emphasized at this point that the sharp increase in the heat of sorption for DMP and DMH as a function of coverage has not been observed in other molecular sieves. Although intermolecular attractions induce an increase in the heat of adsorption with coverage for wide-pore zeolites, such an increase never exceeded the heat of condensation of the alkanes sorbed.[24] In the present case, the difference between the heat of adsorption at low and moderate coverage exceeds this by far. The very low heat of adsorption at the initial stages suggests that the adsorption takes place completely at the outside of the zeolite crystallite. This is strongly supported by the fact that the isosteric heat of adsorption of hexane on macroporous materials such as γ-alumina is approximately 25 kJ/mol.[25] Apparently, it is thermodynamically favorable to adsorb the longer hydrocarbon part parallel to the crystallite surface. This parallel sorption structure would account for about 6×10^{18} molecule/g, which corresponds to about 0.5 molecule/pore-mouth acid site. The coverage revealing the largest heat of

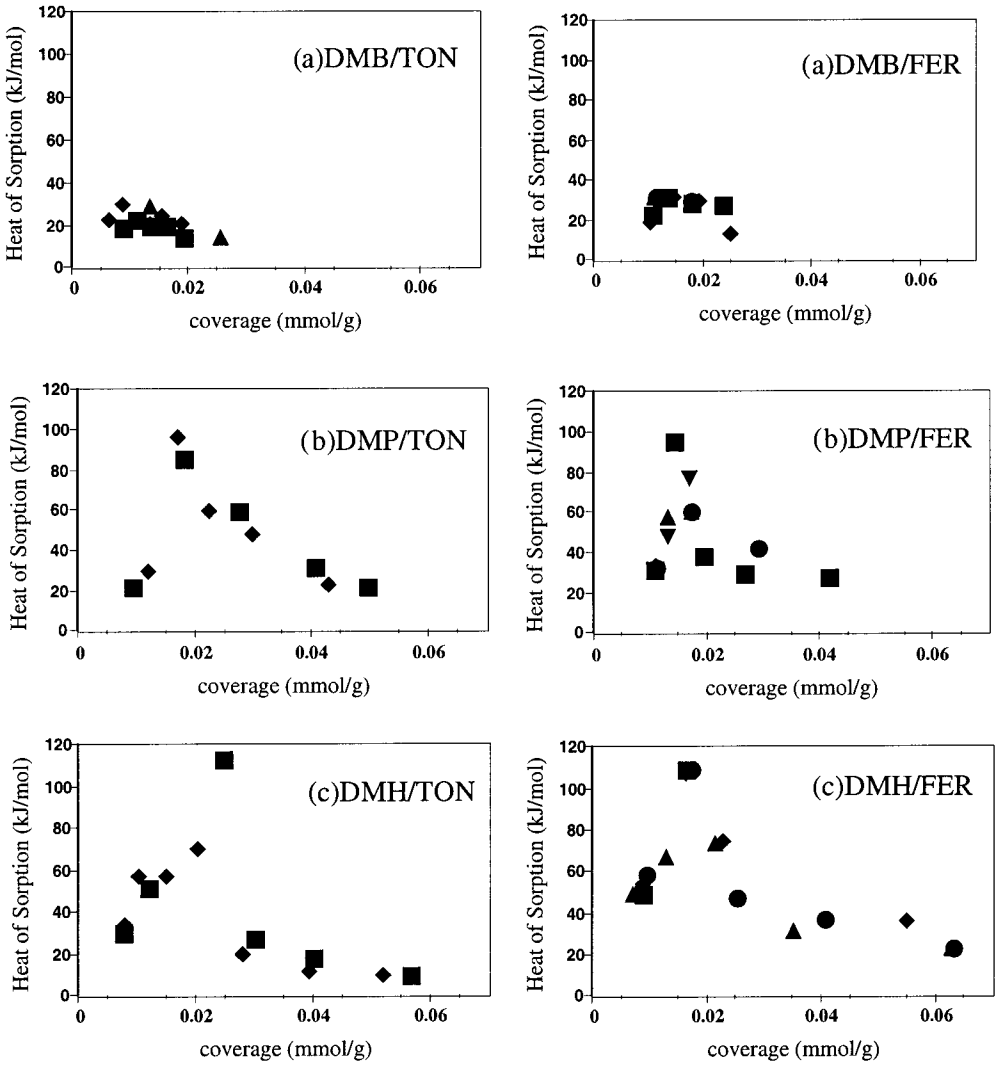

Figure 7. Differential heat of sorption on TON and FER as function of coverage at 343 K for (a) 2,2-dimethylbutane, (b) 2,2-dimethylpentane, and (c) 2,2-dimethylhexane. Different symbols represent independent measurements.

sorption corresponds to roughly 1.2×10^{19} molecules/g. corresponding to about 1 molecule/pore-mouth acid site. Thus, as the coverage increases, additional molecules of DMP and DMH sorb in a way that a much greater heat of adsorption is generated. To account for this, we suggest that additional molecules no longer sorb parallel to the surface but rather protrude into the TON channels, which would indeed lead to a much greater heat of sorption. However, this still is inappropriate to account for the total gain in sorption energy at a coverage that is only twice as much as the initial coverage with low energy. The increase brought about by additional molecules having their sorption structure changed from parallel to the surface to along the direction of the pore would amount to approximately the enthalpy that the *n*-alkane tail generates after adsorption in TON and FER, corresponding to the contribution by four CH_3/CH_2 groups, i.e., to 48−60 kJ/mol.[5] The fact that the observed increase exceeds this value is explained by the contribution of direct bonding to a Brønsted acidic hydroxyl group (estimated contribution of 10 kJ/mol) and by the fact that the majority of the molecules initially sorbed with the parallel sorption structure rearrange their sorption structure from being adsorbed parallel to the surface to pointing into the pore mouths, i.e., adopting the sorption structure of the later-adsorbed alkanes.

The in situ IR (difference) spectra during the adsorption (see Figures 8−10) confirm these conclusions. The IR spectrum of activated TON shows bands at 3740 and 3603 cm^{-1}, which are attributed to the terminal and bridging OH groups, respectively. Upon sorption of DMB at increasing equilibrium pressure, the intensities of both bands decreased simultaneously, and a single broad band characteristic of hydrogen bridge bonding to the alkane appeared at lower wavenumbers. In contrast to those of DMB, the spectra during sorption of DMP and DMH clearly show a distinct difference between low and high coverages. At the lowest loadings (below 0.02 mmol/g), a small shift toward lower wavenumber in the band of the bridging hydroxyl groups (40−60 cm^{-1}) was observed, indicating weak interactions with a methyl group. At higher coverage, a larger downward shift of the bridging hydroxyl groups was seen, i.e., 140 cm^{-1} for DMP and 145 cm^{-1} for DMH. Note that the wavenumber of the perturbed OH group indicates the strength of the interaction, and hence, the increasing shift points to a greater strength.[26] The shift of the free Si−OH−Al group was only 95 cm^{-1} in the case of DMB, and this nonproportionally lower value confirms the strikingly lower heat of sorption in comparison with those of the other alkanes. At low coverage, the uptake of hydrocarbons corresponded fairly well to the decrease of the band of the free hydroxyl groups. When more than about 3% (DMB) to 6% (DMP and DMH) of the total Brønsted acid sites interacted with hydrocarbons, the concentration of sorbed alkanes exceeded the stoichiometry of one molecule per pore-mouth acid site indicating that the additional molecules adsorbed outside the pore mouth. The occurrence of a 1-to-1 stoichiometry

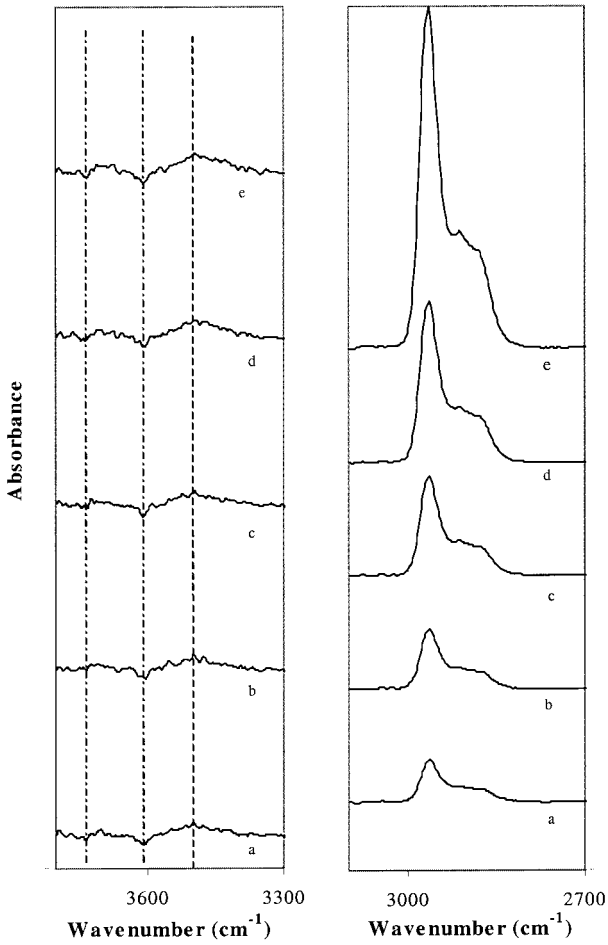

Figure 8. IR spectra of TON during sorption of DMB (343 K). The signals correspond to increasing (a −e) equilibrium pressures between (a) 0.01 and (e) 10 mbar of DMB. The straight lines mark the 3740 cm^{-1} and 3603 cm^{-1} bands (- − - − -) and the perturbation of the 3603 cm^{-1} band (− − −).

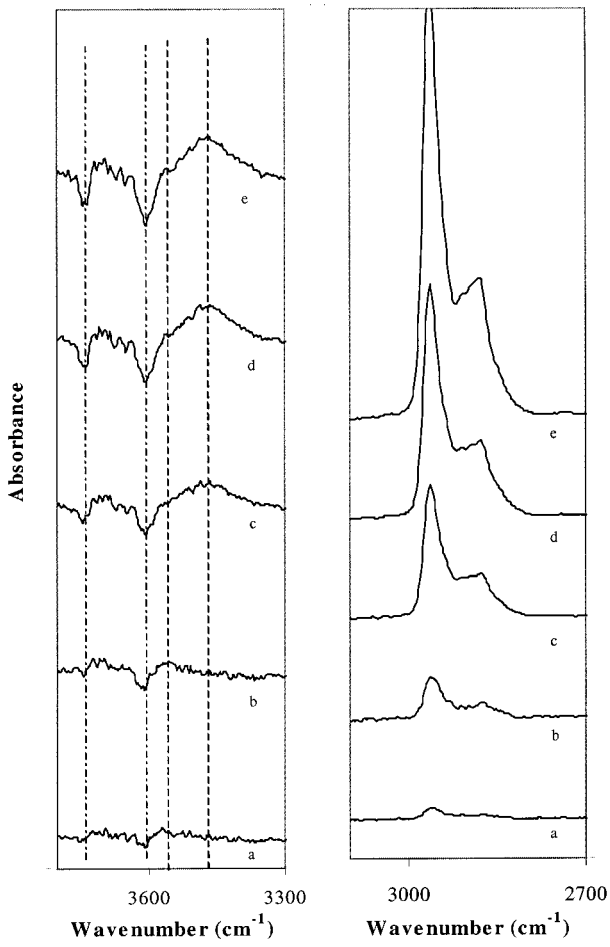

Figure 9. IR spectra of TON during sorption of DMP (343 K). The signals correspond to increasing (a−e) equilibrium pressures between (a) 0.01 and (e) 10 mbar of DMP. The straight lines mark the 3740 cm^{-1} and 3603 cm^{-1} bands (- − - − -) and the perturbation of the 3603 cm^{-1} band (− − −).

also suggests that the defect structure of the rim of the zeolite crystals does not affect the adsorption behavior to any significant extent. Although the relative number of Lewis acid sites (indicative of the aluminum oxide clusters in a nonframework position) on TON clearly exceeds the number found for FER, the adsorption characteristics for dibranched alkanes were essentially similar for both the zeolites.

We suggest that the branched alkanes sorb first on the surface of the zeolite crystals in such a manner that one of the methyl groups points into the pore mouth, while the rest of the molecule is sorbed in parallel to the external crystal face. With DMB, the difference between the methyl and the ethyl group is so small that it is hardly noticeable. Most likely, there is a rapid redistribution between the two forms of adsorption. Moreover, it should be kept in mind that the adsorption form parallel to the surface will have a greater entropy in the adsorbed state and might, therefore, be preferred. For DMP and DMH, the gain in enthalpy at higher loadings clearly outweighs the loss of entropy, and a strict ordering of the longer alkane chain into the pore mouth occurs. The differences in the maximum heats of adsorption for DMP and DMH (13−16 kJ/mol) are in the range of the values found for the adsorption of linear and singly branched alkanes,[6,23] i.e., one additional methylene group will contribute about 12 kJ/mol to the overall heat of sorption. Therefore, we think that the arrangement of the longer part of the dibranched alkane is very similar to the arrangement of the linear alkane in the optimized conformation.

The adsorption structure at the pore mouth/external surface seems, thus, to be related to the size of the alkane. However, the conditions of adsorption may also affect the adsorption structure. In two recent papers, Denayer et al. used tracer chromatography and perturbation chromatography at catalytic working temperatures to determine adsorption characteristics on ZSM22 (TON).[28,29] The work of Denayer et al. deals with linear and branched alkanes. Among the branched alkanes, 2,2-dimethylbutane and 3,3-dimethylpentane are the two molecules that have dibranching at the same carbon atom. On the basis of the capacities, adsorption enthalpies, and adsorption entropies, these authors drew essentially the same conclusions concerning pore-mouth adsorption of branched alkanes with the linear hydrocarbon part penetrating into the pore. However, the parallel adsorption mode was not observed at high temperature. Although one could conclude from this that the adsorption structure is dependent on the temperature of adsorption, the size of the protruding part of the alkane seems important too. We show in our case that, among the dibranched molecules, only 2,2-DMP and 2,2-DMH rearrange as a function of the coverage, with their propyl or butyl chain protruding into the pore. In the case of 2,2-DMB, in line with the results of Denayer, this rearrangement was not observed. As noted above, the reason for this could be that either a methyl or an ethyl group protrudes into the pore mouth and, in either case, the difference gained in stability is only marginal. Hence, this effect is only seen in the type of molecules with longer chains with dibranching.

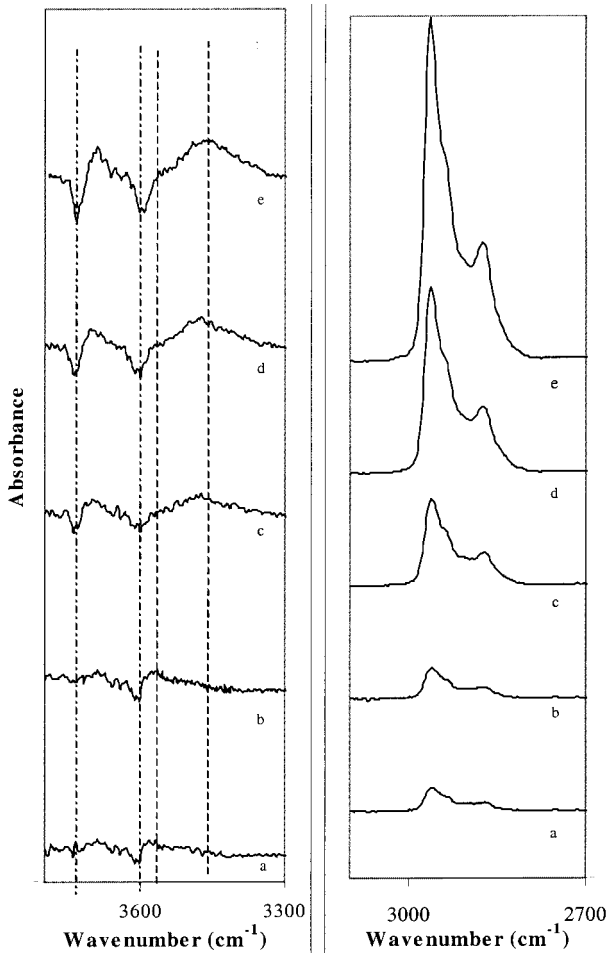

Figure 10. IR spectra of TON during sorption of DMH (343 K). The signals correspond to increasing (a−e) equilibrium pressures between (a) 0.01 and (e) 10 mbar of DMH. The straight lines mark the 3740 cm^{-1} and 3603 cm^{-1} bands (- − - − -) and the perturbation of the 3603 cm^{-1} band (− − −).

Conclusions

The sorption of dibranched alkanes and methyl-substituted pyridines in the medium-pore zeolites FER and TON has been investigated by means of in situ IR spectroscopy and combined calorimetry and gravimetry. The accessibility of Brønsted acid sites for dibranched alkanes is established by probing the acid sites with (substituted) pyridine. For both zeolites, the uptake of the dibranched alkanes was small compared to that of the linear molecules. The orientation of the sorbate seems to depend subtly on the size of the molecule. At low coverages, all three dimethylalkanes are adsorbed in parallel to the outer surface of the zeolite. As the coverage increases, additional molecules sorb in such a manner that the propyl and butyl groups point into the pore. Approximately 80% of the 2,2-dimethylpentane and 2,2-dimethylhexane molecules that initially sorbed parallel to the outer surface rearrange to this sorption structure. With 2,2-dimethylbutane, a clear differentiation is not possible with the present data. The adsorption at the pore mouth involves strong Brønsted acid sites, as shown directly by in situ IR measurements that also allow one to follow the rearrangement of the dibranched molecules. The strong Brønsted acid sites (sufficiently strong to convert alkanes and alkenes in skeletal isomerization) are, therefore, concluded to be located in the pore mouth rather than on the outside of the zeolite crystal. The defect structure of the rim of the zeolite crystals of TON and FER does not affect the adsorption behavior to any significant extent.

Acknowledgment. This work was performed under auspices of NIOK, the Netherlands Institute for Catalysis Research. The fruitful discussions with and the provision of the dibranched alkanes by Prof. J. Martens and Prof. P. Jacobs, University of Leuven, Leuven, Belgium, were highly appreciated. Dr. Làszlò Domokos is kindly acknowledged for assistance concerning the MSI software. We are grateful to Dr. M. Derewinski for providing the TON sample. J.A.Z. Pieterse is indebted to S.O.N/N.W.O. for financial support.

References and Notes

(1) Mooiweer, H. H.; de Jong, K. P.; Kraushaar-Czarnetzki, B.; Stork, W. H. J.; Krutzen, B. C. H. *Stud. Surf. Sci. Catal*. **1996**, *84*, 2327.
(2) Houzvicka, J.; Ponec, V. *Catal. Rev.−Sci. Eng*. **1997**, *39* (4), 319.
(3) Kärger, J.; Petzold, M.; Pfeifer, H.; Ernst, S.; Weitkamp, J. *J. Catal*. **1992**, *136*, 283.
(4) Martens, J. A.; Souverijns, W.; Verrelst, W.; Parton, R.; Froment, G. F.; Jacobs, P. A. *Angew. Chem., Int. Ed. Engl*. **1995**, *107*, 2726.
(5) Eder, F.; Lercher, J. A. *J. Phys. Chem. B* **1997**, *101*, 1273.
(6) Meier, W. M.; Olson, D. H. *Atlas of Zeolite Structure Types*; Butterworth-Heinemann: London, 1992.
(7) Morris, R. E.; Weigel, S. J.; Henson, N. J.; Bull, L. M.; Janicke, M. T.; Chmelka, B. F.; Cheetman, A. K. *J. Am. Chem. Soc*. **1994**, *116*, 11854.
(8) Knözinger, H. In *Elementary Reaction Steps in Heterogeneous Catalysis*; Joyner, R. W., Santen, R. V., Eds.; Kluwer Academic Publishers: New York, 1993; p 267.
(9) Khabtou, S.; Chevreau, T.; Lavalley, J. C. *Microporous Mater*. **1994**, *3*, 133.
(10) Knözinger, H.; Krietenbrink, H.; Ratnasamy, P. *J. Catal*. **1977**, *48*, 436.
(11) Buzzoni, R.; Bordiga, S.; Ricchiardi, G.; Lamberti, C.; Zecchina, A. *Langmuir* **1996**, *12*, 930.
(12) Benesi, H. A. *J. Catal*. **1973**, *28*, 176.
(13) Jolly, S.; Saussey, J.; Lavelley, J. C.; Zanier, N.; Benazzi, E.; Joly, J. F. *Ber. Bunsen-Ges.* **1993**, *97*, 3.
(14) Glazunov, V. P.; Odinokov, S. E. *Spectrochim. Acta* **1982**, *38A*, 399.
(15) Dewing, J.; Monks, G. T.; Youll, B. *J. Catal*. **1976**, *44*, 2.
(16) Matulewicz, E. R. A.; Kerkhof, F. P. J. M.; Moulijn, J. A.; Reitsma, H. J. *J. Colloid Interface Sci.* **1980**, *77*, 110.
(17) Corma, A.; Rodellas, C.; Fornes, V. *J. Catal*. **1984**, *88*, 374.
(18) Jacobs, P. A.; Heylen, C. F. *J. Catal*. **1974**, *34*, 267.
(19) Deka, R.; Vetrivel, R. *J. Catal*. **1998**, *174*, 88 and references therein.
(20) Barrer, R. M. *J. Colloid Interface Sci*. **1966**, *31*, 415.
(21) Derouane, E. G.; Andre, J. M.; Lucas, A. A. *J. Catal*. **1988**, *110*, 58.
(22) Eder, F.; Stockenhuber, M.; Lercher, J. A. *Stud. Surf. Sci. Catal*. **1995**, *97*, 495.
(23) Van Well, W. J. M.; Cottin, X.; de Haan, J. W.; Smit, B.; Nivarthy, G. S.; Lercher, J. A.; van Hooff, J. H. C.; van Santen, R. A. *J. Phys. Chem.* **1998**, *102*, 3945.
(24) Eder, F.; Lercher, J. A. *Zeolites* **1997**, *18*, 75.
(25) Baumgarten, E.; Weinstrauch, F.; Höffkes, H. *J. Chromatography* **1977**, *138*, 347.
(26) Hair, M. L.; Ertl, W. *J. Phys. Chem*. **1970**, *74*, 91.
(27) Insight II program, Molecular Simulations Inc., San Diego, CA, 1998.
(28) Denayer, J. F.; Souverijns, W.; Jacobs, P. A.; Martens, J. A.; Baron, G. F. *J. Phys. Chem. B* **1998**, *102*, 4588.
(29) Denayer, J. F.; Baron, G. F.; Vanbutsele, G.; Jacobs, P. A.; Martens, J. A. *Chem. Eng. Sci.* **1999**, *54*, 3553.